2013 IEEE/RSJ International Conference on
Intelligent Robots and Systems (IROS)
November 3-7, 2013. Tokyo, Japan

Energy-Consistent Haptic Rendering of Contact Forces

Arash Mohtat and József Kövecses

Abstract— **Enhancing the realism of the perceived contact force is a primary challenge in haptic rendering of virtual walls (VWs) and objects (VOs). For VOs, this goal directly translates into accurate rendering of not only stiffness, but also mass. The most challenging situation arises when the stiffness of the object is large, its mass is small, and sampling is slow. To address this challenge, a framework entitled *high-fidelity haptic rendering* (HFCR) has been developed. The HFCR framework is composed of the following three main strategies: an energy-consistent rendering of the contact force, smooth transition between contact modes, and remaining leak dissipation. The essence of all these strategies is to make the energy of the VO emulate its continuous-time counterpart. This is achieved through physically meaningful modifications in the constitutive relations to suppress artificial energy leaks. This paper reports simulation and experiments involving the one-dimensional canonical model of a VO to illustrate the HFCR framework and compare it to the existing methods. Results demonstrate the promising stability and force rendering fidelity of this framework.**

I. Introduction

Rendering realistic contact forces is the key to satisfactory haptic interaction with virtual objects (VOs). Increasing the perceived rigidity of the VO while accurately displaying its mass is the core challenge in this context. This should be accomplished at the available sampling rate, which might be low depending on the computational resources. Ref. [1] offers a good overview of contact modeling methods and classifies them into three groups: impulse-based, constraint-based, and penalty-based techniques. According to it, impulse-based techniques produce results which are visually acceptable but poor in terms of haptic feedback for sustained contacts and dry friction [2]. Many of the constraint-based techniques, on the other hand, rely on variable step integrators [3] or fixed step-compatible algorithms with no guaranteed completion time [4] that are not useful for haptic applications. When adapted to accommodate haptic application requirements, the potential advantage of perfectly rigid contact due to exact enforcement of constraints is lost [5], [6]. Penalty-based methods [7] seem to be directly applicable and useful in haptics; but, to achieve high perceived rigidity, high stiffness values are required which compromise stability when implemented digitally. In this study, only the basic interaction in one direction is considered to facilitate focusing on the fundamental discrete-time constitutive law of penalty-based contacts.

Both authors are with the Department of Mechanical Engineering and Centre for Intelligent Machines, McGill University, Montreal, Québec, Canada, E-mails: amohtat@cim.mcgill.ca and jozsef.kovecses@mcgill.ca

Instability issues would not occur if the physical haptic device were interacting with physical objects (which are passive); but, they do arise when interacting with digitally rendered VOs. In the haptics and sampled-data systems literature [8], [9], this phenomenon is referred to as passivity-violating energy leaks. To avoid instability of the haptic system, the energy leaks should be prevented from being accumulated. Most studies have proposed improving virtual dissipation through either replacing the backward differentiation by an enhanced velocity estimation [10], or introducing an additional adaptive dissipative term. A considerable amount of research has been devoted to the latter trend, from the seminal work [11] which introduces the basic passivity-observer passivity-controller (POPC) method to recent investigations that extend its applicability [12]. The time-varying damping adapted through energy observation adds some dynamics that does not have a simple physical interpretation and cannot be easily analyzed. Avoidance of impulsive (sudden) reactions is not guaranteed, even in the case of reference energy following [13] smoothening. This may lead to either fidelity degradation or chattering issues. With special regard to contact rendering, there are two other important issues that have been overlooked in many investigations. Firstly, there are few investigations that directly address the unilaterality of contact. Obviously, delayed activation or deactivation of contacts leads to energy leaks that cannot be neglected in challenging situations. Such leaks are not automatically detected with passivity observers, for instance. Ref. [14] is an example that identifies this issue. The scenario addressed in that work involves collision of a virtual mass to a virtual wall (VW). The energy leak produced in such a situation is internal to the virtual world, and there is more freedom for handling it. The case of interest in the current study is a little different; and, involves unilateral contact of the physical device with a VO. The second issue is that there has been too much emphasis on VWs; and, interaction with VOs of possibly finite mass has not received enough attention. Investigations on rendering mass are few. In fact, Ref. [15] from 1998 still remains one of the key references in this area. This work discusses simply a finite mass attached to the device through a classic virtual coupling (without unilateral contact). Actually, the importance of this work is not in the methods it presents, but in the fundamental groundwork that it lays down, especially: the proofs of non-existence of passive discrete-time integrators and the existence of a minimum renderable virtual mass.

To address the aforementioned issues, in this paper, a framework has been developed which is entitled as *high-fidelity contact rendering* (HFCR). For illustration purpose,

978-1-4673-6357-0/13/$31.00 ©2013 IEEE

this framework has been worked out in 3 steps: each introducing a clear modification to the basic approach. The assumptions and the basic approach have been reviewed in section II. The three steps are developed in subsections III-A through III-C. Section IV is devoted to experimental validation. We have experimentally compared our method against a number of available methods in the literature, including: the virtual coupling [15]; the sample-estimate-hold method [16]; and, the passivity controller with reference energy following [13]. Simulation and experimental results demonstrate that the HFCR is a promising framework to increase the range of renderable contact situations.

II. Background

This section presents the basic approach to contact rendering, i.e. employing a two-mode model which considers the VO in either free-motion or contact with the device. Subsection II-A reviews the constitutive law for contact rendering and introduces the nondimensionalized stiffness pair; while, subsection II-B develops this basic two-mode canonical model.

A. Constitutive Law of Contact

The constitutive law of contact is:

$$f^c = fh(p) \tag{1}$$

where f^c is the contact force; $h(p)$ imposes the unilaterality of contact with the unit step function $h(.)$ and the penetration p into the object; and, f is referred to as the interaction force. In case of penalty-based contact modeling, the interaction force is defined with the constitutive law:

$$f = Kp + B\dot{p} \tag{2}$$

where K and B are the stiffness and damping coefficients penalizing penetration and its rate, respectively. For the purpose of haptic contact rendering, a discretized version of (2) is required. Throughout this study, we assume availability of only position-level measurements of the device through an ideal sampler. As a result, the penetration coordinate is only known at the sampling instants; while, its rate should be estimated. It is also assumed that the contact force is fed back to the haptic device through a zero-order hold (ZOH). Under these assumptions, the most handy discretized version of (2) is:

$$f_i = Kp_i + B\frac{p_i - p_{i-1}}{T} \tag{3}$$

where T is the sampling period. The first term on the RHS is known as a virtual spring (VS), and the second as a virtual damper (VD). Using this constitutive law, the sustained contact of the haptic device end-point with a VO is equivalent to a classic virtual coupling [15]. Such a digital rendering of contact with VOs leads to energy leaks and potential instability issues. There are two prominent issues with Eq. (3):

1) No information about the mass of the VO has been incorporated. This means no provision for the additional challenge in rendering lighter VOs.

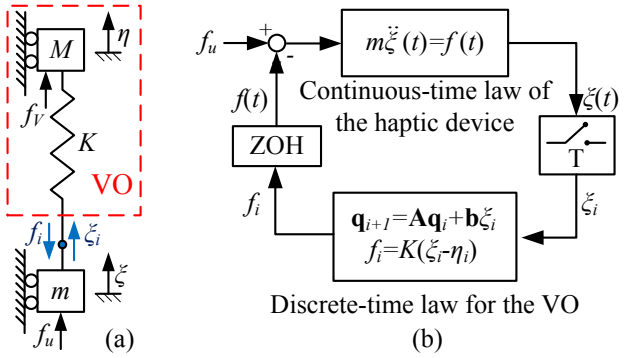

Fig. 1: The VS-VM system for modeling the VO in contact mode: schematic (a); and, block-diagram (b).

2) Even in the case of a VO of infinite mass, i.e. a virtual wall (VW), the VS term produces major energy leaks proportional to KT^2 in each sampling interval.

Most studies have avoided addressing these two problems directly and have focused on improving the damping term, instead. This has been done through either enhanced velocity estimation [10], or time-domain passivity methods [11]–[13], [17], [18]. In this paper, however, we will tackle directly the aforementioned problems (section III-A). The unilaterality of contact will also be explicitly addressed (section III-B). At the end, a minimal amount of dissipation will be added to dissipate the inevitable small remaining leaks (section III-C). This will be shown to be advantageous over the previous methods that attempt to dissipate major energy leaks, only after allowing them to be generated.

B. The Basic 1-D Canonical Model for a VO

A generic scenario involving one-dimensional contact interaction of a VO with a haptic device is considered in this paper. The VO has a mass of M and stiffness of K; and, is under the effect of an arbitrary virtual force f_V and the force f exerted from the haptic device. Note that $-f$ is the reaction to the haptic device, and the force feedback supposed to be rendered. We designate f as the rendering force, and we apply the negative sign in the feedback interconnection as will be discussed shortly after (see Fig. 1). The device is modeled as an undamped physical mass m driven by the user force f_u. Note that this selection of the haptic device is only for purpose of numerical simulation. In fact, the contact rendering methods developed in this paper do not depend on any haptic device model, but only on the VO model.

The basic model for the VO has two modes: free-motion, and contact. The latter is schematically shown in Fig. 1a. The free-motion mode can also be represented by the same sketch with the VS deleted. Mathematically, it is described by $\ddot{\eta} = f_V/M$ in the interval $I_i = [t_i, t_{i+1})$, subject to initial conditions: $\eta(t_i) = \eta_i$ and $\dot{\eta}(t_i) = \dot{\eta}_i$. A straight-forward integration leads to:

$$\mathbf{q}_{i+1} = \begin{bmatrix} 1 & T \\ 0 & 1 \end{bmatrix} \mathbf{q}_i + \begin{bmatrix} \frac{\alpha_i}{2} T^2 \\ \alpha_i T \end{bmatrix} \tag{4}$$
$$f_i = 0$$

where $\alpha_i = f_{V,i}/M$; $\mathbf{q}_i = [\eta_i, \dot{\eta}_i]^T$ is the state vector including the position and velocity of the VO; and, f_i is the force fed back to the haptic device during I_i (zero in free-motion). Contact is activated when a positive penetration $p_i = \xi_i - \eta_i$ is detected between the VO and the haptic device end-point. Such an occurrence triggers switching to the contact mode in which the VO becomes a VS-VM (virtual spring and mass) system, see Fig. 1a.[1] During the interval I_i, the VS-VM receives the device position measurement ξ_i and outputs a force f_i. This force is held constant and fed back to the haptic device through the ZOH. Fig. 1b shows the block-diagram of this interconnection which uses the negative feedback convention. The VS-VM is supposed to emulate its continuous-time counterpart which is described by the following differential equation in the interval $t \in I_i$:

$$M\ddot{\eta}(t) - f_V(t) = K\xi(t) - K\eta(t) = f(t) \tag{5}$$

subject to $\eta(t_i) = \eta_i$ and $\dot{\eta}(t_i) = \dot{\eta}_i$ as initial conditions. Assuming the sampled values ξ_i and $f_{V,i}$, the solution to this initial condition problem is:

$$\eta(t) = \frac{\dot{\eta}_i}{\Omega}\sin[\Omega(t-t_i)] + (\eta_i - \zeta_i)\cos[\Omega(t-t_i)] + \zeta_i$$

where $\Omega = \sqrt{K/M}$, and $\zeta_i = \xi_i + \frac{\alpha_i}{\Omega^2}$. Recursions for updating the state vector $\mathbf{q}_i$ of the VM based on this solution lead to the following discrete-time model:

$$\mathbf{q}_{i+1} = \mathbf{A}(T)\mathbf{q}_i + \mathbf{b}(T)\zeta_i \tag{6a}$$
$$f_i = K(\xi_i - \eta_i) \tag{6b}$$

where

$$\mathbf{A}(T) = \begin{bmatrix} \cos(\Omega T) & \frac{1}{\Omega}\sin(\Omega T) \\ -\Omega\sin(\Omega T) & \cos(\Omega T) \end{bmatrix}, \mathbf{b}(T) = \begin{bmatrix} 1-\cos(\Omega T) \\ \Omega\sin(\Omega T) \end{bmatrix};$$

and, the elastic ($B = 0$) interaction law (3) has been used for rendering the contact force.

A simple numerical experiment with this basic two-mode model reveals that it does not render contacts satisfactorily. The numerical values of the parameters are chosen as: $m = M = 0.1$, $K = 100$, $T = 0.01$, $g = 9.81$, $f_V = -Mg$, $f_u = mg$, $\xi_0 = 0$, $\eta_0 = 0.1$, and $\dot{\xi}_0 = \dot{\eta}_0 = 0$ (all SI units). This example represents a VO falling due to gravity and bouncing on a virtual rigid plate underneath. The rigid plate is attached to the EP of the haptic device which enables feeling the bouncings of the VO. The simulation is run using a sufficiently small time-step ($\delta t = 1 \times 10^{-5}$) to capture the intersample behavior. The ideal result is obtained by setting $T = \delta t$, as if the haptic device were interacting with the physical counterpart of the VO. As shown in Fig. 2, the VO rendered via the basic model is very unstable.

III. High-Fidelity Contact Rendering

In this section, we develop the HFCR framework in three steps, then we compare the results with some other methods in the literature.

[1]Note that in this figure, the VS is just a graphical visualization of the concept; hence, we do not need to associate a length to the spring.

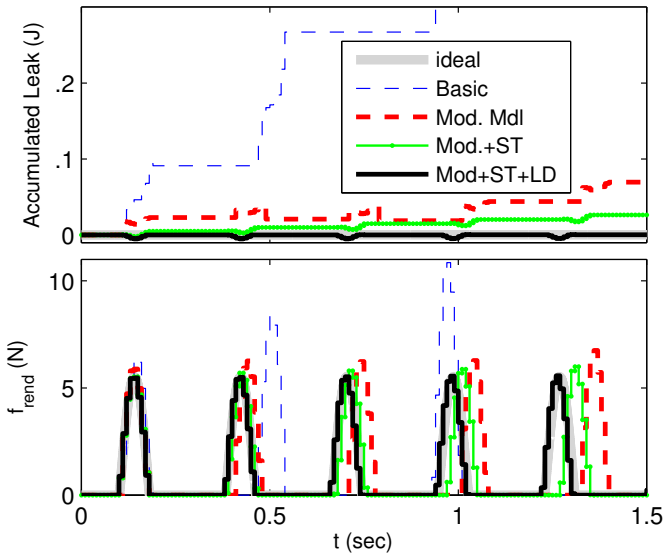

Fig. 2: The VO simulation example: step-by-step development of the HFCR (Mod+ST+LD) framework.

A. Modified Contact

In this subsection, we improve the contact mode of the basic model by modifying the contact force (6a) through an energy-based derivation. In fact, the ideal force f_i^{ideal} to be fed to the haptic device through the ZOH should satisfy the following energy balance over I_i:

$$-f_i^{ideal}(\xi_{i+1} - \xi_i) = -(S_{i+1} - S_i) \tag{7}$$

where the LHS is the work done by $-f_i^{ideal}$ on the device (notice the negative feedback convention, see Fig. 1b); and, the RHS is the negative of the change in the stored energy of the VS-VM system. At any instant t_j, the stored energy S_j consists of the kinetic energy and possibly (if $\xi_j - \eta_j > 0$) the spring potential:

$$S_j = \frac{M}{2}\dot{\eta}_j^2 + \frac{K}{2}(\xi_j - \eta_j)^2 h(\xi_j - \eta_j) \tag{8}$$

Based on Eq. (7), f_i^{ideal} cannot be exactly computed at t_i; instead, it will be approximated by:

$$f_i^{mod} = \frac{\tilde{S}_{i+1} - S_i}{\tilde{\xi}_{i+1} - \xi_i} \tag{9}$$

where the tilde signs represent one-step ahead prediction. The constant mean velocity approximation,[2] yields: $\xi_{i+1} \approx \tilde{\xi}_{i+1} = 2\xi_i - \xi_{i-1}$. This approximation will be also used in the computation of $\tilde{S}_{i+1}$:

$$\tilde{S}_{i+1} = \frac{M}{2}\dot{\eta}_{i+1}^2 + \frac{K}{2}(\tilde{\xi}_{i+1} - \eta_{i+1})^2 h(\tilde{\xi}_{i+1} - \eta_{i+1})$$

where η_{i+1} and $\dot{\eta}_{i+1}$ are computed according to Eq. (6a) using only the quantities at t_i.

[2]In haptics, model-based prediction of velocity is not very useful, mainly due to the unknown influence of the user. Other possibilities are the constant mean velocity approximation and extrapolation [12]. We will use the simplest approximation, and deal with the remaining leaks afterwards.

Any approximation f_i^* to f_i^{ideal} creates an error in the energy balance (7) over I_i which is called an energy leak. (9)

$$L^*[I_i] = S_{i+1} - S_i - (\xi_{i+1} - \xi_i) f_i^* \tag{10}$$

To avoid confusion hereafter, L^* is denoted by L^{ognl} (original leak) and L^{rem} (remaining leak) when f_i^* is computed based on f_i (6b) and f_i^{mod} (9), respectively. In Ref. [19], it is proven that L^{rem} is smaller than L^{ognl} by at least one order-of-magnitude. It is possible to keep track of these leaks and their accumulation, since $L^*[I_i]$ can be exactly computed in the next interval (at t_{i+1}). Fig. 2 shows the result of employing the modified model composed of Eqs. (6a) and (9). The improvement in the force rendering fidelity is clear; and, the accumulated value (summation over all intervals) of L^{ognl} and L^{rem} can be easily compared. Although L^{rem} is significantly decreased; the accumulated value is still growing. This shows that further improvement of the model is still required as will be discussed in the following subsections.

B. Smooth Transition

At extreme contact situations, each collision event spans only few sampling intervals (e.g. see the second experiment in section IV). Contact transition at intersample points is only detected at the next sampling instant. This may lead to significant energy leaks considering the significance of the contact activation/deactivation time delay relative to the overall duration of each collision event. The previous model entails only two modes, thus is vulnerable to this issue. This is what we intend to improve here by introducing smooth transition (ST). At each instant t_i, the VO could be in either free motion if $p_i < 0$ ($p_i = \xi_i - \eta_i$ is the penetration coordinate), otherwise in contact. The sampling interval $I_i = [t_i, t_i + T)$ could be spent either sustaining the mode or transiting to the other. In case of sustainment of the mode, the appropriate continuous-time dynamic equations can be integrated over a period of T seconds to yield the state-update equations of the corresponding mode, i.e. either (4) or (6a). In case of mode transition, the transition instant τ_i should be estimated by solving $\tilde{p}(t_i + \tau_i) = 0$. This equation can be solved numerically assuming constant mean velocity for the position of the haptic device end-point, and using the appropriate position-update for the VO (according to either free-motion or contact depending on the transition case). The states are then updated based on two appropriate consecutive updates of τ_i and $T - \tau_i$ seconds. In case of free-motion sustainment, the contact force is zero; while, in all other cases, can be rendered through (9). Note that since the actuation frequency is the same as the sampling, there is no possibility to render zero and nonzero forces in the τ_i and $T - \tau_i$ subintervals. Interestingly, there is no need for such a thing; and, Eq. (9) automatically provides an energetically-equivalent[3] constant value to be applied in the entire interval.

[3]Note that the energy balance depends only on the two endpoints of the interval, and not the intersample transition. The unit step $h(.)$ in the energy formulation automatically takes into account the predicted contact mode at the two endpoints.

The results of applying this ST, labeled as 'Mod.+ST', are shown in Fig. 2; and, demonstrate improved leak reduction and force fidelity over the modified model without ST. The accumulated leak is still growing, though; and, there is still need for further improvement.

C. Remaining Leak Dissipation

In all the modification proposed so far, there is a need for predicting ξ_{i+1} (the haptic device position at t_{i+1}) using only the information available up to t_i. This prevents from complete suppression of energy leaks, and gives rise to *remaining* leaks. Fortunately, the framework introduced in subsection III-A can alleviate the problem. The remaining leaks in each interval can be evaluated in the next, and their accumulation can be monitored. To suppress remaining leaks, a desired dissipation can be added to the rendering Eq. (9) in the form of:

$$f_i^{mod} = \frac{\tilde{S}_{i+1} - S_i}{\tilde{\xi}_{i+1} - \xi_i} + \frac{\sigma_i}{T} b_i (\dot{\xi}_i - \dot{\eta}_i) \tag{11}$$

where:

$$\sigma_i = \begin{cases} T - \tau_i & : p_i \le 0 \ \ \& \ \ \tilde{p}_{i+1} > 0 \\ \tau_i & : p_i > 0 \ \ \& \ \ \tilde{p}_{i+1} \le 0 \\ T & : p_i > 0 \ \ \& \ \ \tilde{p}_{i+1} > 0 \end{cases}$$

and b_i is a damping coefficient. This can be interpreted as a damper parallel to the VS (see Fig. 1a) that is activated during the contact subinterval σ_i. We have purposefully made a distinction between the virtual damper (VD) coefficient B in Eq. (3) and coefficient b_i. The latter is intended to dissipate only artificial leaks remaining after all the other modifications, without introducing any additional dissipative behavior. Since, these leaks are way smaller than the original leaks, the overall performance of the HFCR method (modified model, plus ST and LD) is not very sensitive to the value of b_i. This is why a roughly tuned fixed value proves to work very well, as shown in Fig. 2. This figure clearly illustrates the relative merit of each part in the overall performance of the HFCR framework. For a non-modified model plus VD, however, a more careful tuning of the B-term is required.

IV. Experimental Validation

The setup used in this study consists of a 2-DOF Quanser Pantograph as the haptic device (see Fig. 3) equipped with two high-resolution optical encoders and actuated by two graphite brush DC motors through a cable-driven mechanism; a QPA-L4-E Power Amplifier; and, a PC equipped with a Quanser Q4 data-acquisition board that is connected to MATLAB/Simulink® via the QuaRC® toolbox.

The experiment involves the interaction of the end-point (EP) of the haptic device with a VO under effect of virtual gravity (see Fig. 3b). Since there is no external force component in the x-direction and the device is symmetric with respect to the y-axis, the EP moves only along the y-axis. Nevertheless, a PID controller is added to enforce the bilateral constraint on the x-direction in case any minor disturbance occurs. To ensure repeatability and reproducibility of the results, the human operator (user) is replaced by

a constant force f_u in the y-direction on the EP, through equivalent torques applied at the actuated joints. The users force is unknown to the rendering algorithms. This implies that, in principle, any other bounded force signal could have been used instead, leading to fairly similar results.[4] Unlike the simulation example, the device is not just a point mass. This does not have any direct impact on the rendering methods, since they are not based on a dynamic model of the device. We only need an approximate effective mass at the EP in the y-direction (about 0.25 kg) to have an idea about the nondimensionalized static stiffness value. A safety switch has been implemented to disconnect the device from the amplifier whenever the EP exits an allowable box in its workspace (corresponding to too much contraction/extension of the arms).

In the first experiment, a VO with a mass of 0.1 kg and a stiffness of 100 N/m is rendered at 50 Hz. Note that although the nominal stiffness is low, this situation is still rather challenging since the sampling is extremely slow. In fact, it is more constructive to consider the nondimensionalized stiffness pair $(\kappa,\mathcal{K}) = (KT^2/m, KT^2/M)$ to assess the rendering difficulty.[5] In this sense, rendering a stiffness of 100 N/m at 50 Hz is equivalent to rendering a stiffness of 40 kN/m at 1 kHz (in terms of original energy leaks). Such a selection of experimental parameters minimizes the effect of issues such as actuator saturation, quantization errors, structural flexibility, etc. that would otherwise diminish the validity of the experimental data. The more important advantage is that there is a way to obtain a very good approximation of the ideal rendering. If we repeat the experiment with the same nominal mass and stiffness values at a higher sampling rate, we can obtain extremely low-leak results that can be used as an ideal reference. Note that at 1 kHz, the artificial leaks

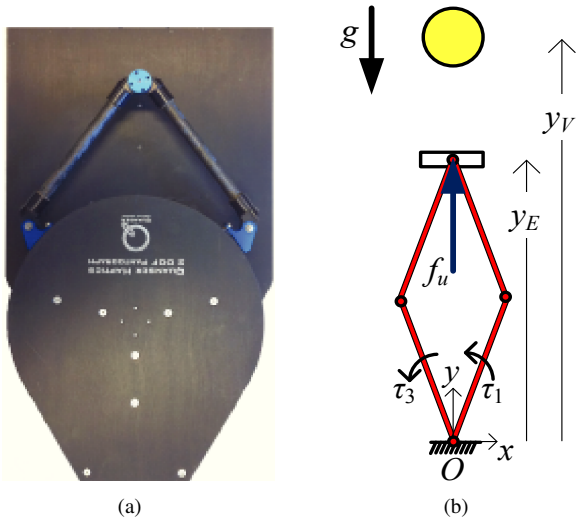

(a) (b)

Fig. 3: (a) The 2DoF haptic device. (b) The experiment.

[4]For more details on the effect of human operator on the stability of the haptic system, refer to Ref. [19].

[5]Parameter m is a reference mass for nondimensionalization (usually selected as the effective mass at the endpoint of the device).

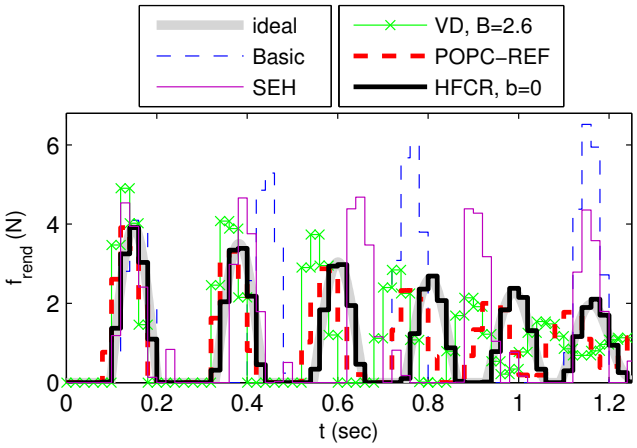

Fig. 4: Experimental results at $\kappa = 0.16$, $\mathcal{K} = 0.4$.

will be about 400 times smaller. The other parameters have been chosen as: $f_V = -Mg$, $g = 9.81$, $f_u = 1$, $\eta_0 - \xi_0 = 0.05$, and $\dot{\eta}_0 = 0$ (all SI units). Note that $\xi = y_E$ where y_E is the y-position of the device EP, computed based on the forward kinematics of the device using the measured angles of the driven joints. Also, $\eta = y_V - r$ where y_V is the y-position of the VO (virtual ball), and $r = 0.01$ is the radius of the ball. Results of implementing the five methods at 50 Hz have been compared in Fig. 4 against the ideal reference obtained by running the basic model at 1 kHz. The five methods are: 1) the basic canonical model (subsection II-B); 2) the basic model corrected by the sample-estimate-hold (SEH) filter [16]; 3) the basic model with a virtual damper (VD) (this is equivalent to a finite mass with a classic spring-damper virtual coupling [15]); 4) the basic model corrected by a passivity-observer passivity-controller with reference energy following (POPC-REF) [13] (a slightly improved implementation of the POPC-REF introduced in Ref. [19] has been used); and, 5) the proposed HFCR method. As expected, the uncorrected basic model leads to instability. The SEH filter produces almost stable results. This is due to the existing physical dissipation of the device. The fidelity, anyhow, is really poor. A VD cannot achieve good fidelity, even when tuned through several trial-and-errors. To gain a quantitative feeling about fidelity, we will use a simple relative RMS-index of the force rendering error (FRE) [19]. The VD, as shown in Fig. 4, achieves only an FRE of 84.9% (computed over the first three collisions). The POPC-REF, however, yields an acceptable fidelity (FRE=51.1%). The HFCR achieves the best rendering (FRE=17.1%) without any damping required.

The stiffness is multiplied by a factor of four in the second experiment. At this extremely high[6] κ and $\mathcal{K}$ values (0.64 and 1.6), the POPC-REF and the VD fail to render the collision events in a stable fashion. In fact, the device exits the allowable workspace after half a second of unsatisfactory

[6]Notice that the difficulty associated with rendering a stiffness of 400 N/m at 50 Hz is equivalent to 160 kN/m at 1 kHz. Also, note that we are rendering a VO of finite mass, and not simply a static VW of infinite mass.

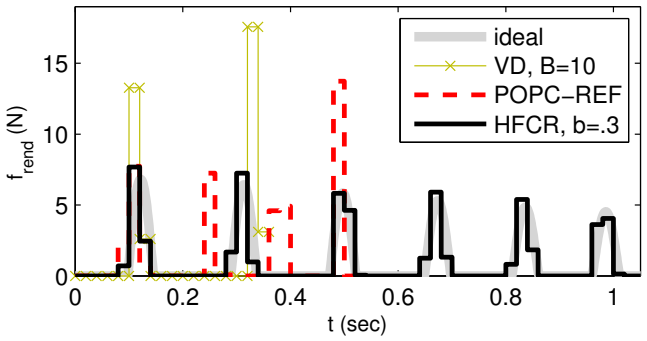

Fig. 5: Experimental results at $\kappa = 0.64$, $\mathcal{K} = 1.6$.

operation in the case of the POPC-REF. And, in the case of the VD, no satisfactory tuning B was found. A representative VD is shown in Fig. 5, using which the safety switch of the device is activated even before completion of the second collision. Using some leak dissipation b, the HFCR enables not only stable rendering; but also, achieves acceptable fidelity. The FRE value over all the six collisions is 52.2%. This is quite impressive considering the nearly extreme situation with each collision event taking only 2 to 3 sampling intervals.

V. Conclusions

A generic framework for *high-fidelity contact rendering* (HFCR) has been developed in this paper. The framework deals with unilateral interaction of a VO with the haptic device in one direction. An impedance-based implementation has been assumed in which the VO receives sampled position-level measurements from the device. The strategies employed in the HFCR framework include an energy-based rendering of the contact force, smooth transition (ST) between contact modes, and remaining leak dissipation (LD). The essence of all these strategies is to improve energy-consistency, i.e. to make the energy of the VO follow its continuous-time counterpart more closely, and to keep energy leaks under control. This is achieved via physically meaningful modifications at the level of constitutive relations.

Our initial experimental results show that the HFCR framework improves fidelity compared to other methods. Also, by allowing for rendering more extreme contact situations, it expands the renderable range of dynamic VOs. Research on characterizing the renderable range of dynamic VOs is underway. In fact, it is possible to describe this range in the nondimensionalized $(\kappa, \mathcal{K})$ stiffness plane, based on stability and passivity considerations. Further future work can involve generalization of the framework to the multi-dimensional case. The energy-consistent rendering (energy-based contact force, plus LD) can be readily generalized using a weighted distribution over the degrees of freedom [19]. Smooth transition in the multidimensional case, however, requires further development with regard to efficient contact detection, and possible multiple-point contact scenarios.

Acknowledgment

The financial support by the Natural Sciences and Engineering Research Council of Canada, Quanser Inc., and the Canadian Space Agency is gratefully acknowledged.

References

[1] D. Constantinescu, S. Salcudean, and E. Croft, "Haptic rendering of rigid contacts using impulsive and penalty forces," *IEEE Transactions on Robotics*, vol. 21, no. 3, pp. 309–323, 2005.

[2] B. Chang and J. Colgate, "Real-time impulse-based simulation of rigid body systems for haptic display," in *1997 ASME Interational Mechanical Engineering Congress and Exhibition*, 1997, pp. 200–209.

[3] D. Baraff, "Analytical methods for dynamic simulation of non-penetrating rigid bodies," in *ACM SIGGRAPH Computer Graphics*, vol. 23, no. 3. ACM, 1989, pp. 223–232.

[4] M. Anitescu and F. Potra, "Formulating dynamic multi-rigid-body contact problems with friction as solvable linear complementarity problems," *Nonlinear Dynamics*, vol. 14, no. 3, pp. 231–247, 1997.

[5] C. Zilles and J. Salisbury, "A constraint-based god-object method for haptic display," in *1995 IEEE/RSJ International Conference on Intelligent Robots and Systems (IROS)*, vol. 3. IEEE, 1995, pp. 146–151.

[6] D. Ruspini and O. Khatib, "Dynamic models for haptic rendering systems," in *Advances in Robot Kinematics: ARK98*, Salzburg, Austria, 1998, pp. 523–532.

[7] A. Gregory, A. Mascarenhas, S. Ehmann, M. Lin, and D. Manocha, "Six degree-of-freedom haptic display of polygonal models," in *Proceedings of the conference on Visualization*. IEEE Computer Society Press, 2000, pp. 139–146.

[8] J. Colgate and G. Schenkel, "Passivity of a class of sampled-data systems: Application to haptic interfaces," in *American Control Conference, 1994*, vol. 3. IEEE, 1994, pp. 3236–3240.

[9] N. Diolaiti, G. Niemeyer, F. Barbagli, and J. Salisbury, "Stability of haptic rendering: Discretization, quantization, time delay, and Coulomb effects," *IEEE Transactions on Robotics*, vol. 22, no. 2, pp. 256–268, 2006.

[10] F. Janabi-Sharifi, V. Hayward, and C. Chen, "Discrete-time adaptive windowing for velocity estimation," *IEEE Transactions on Control Systems Technology*, vol. 8, no. 6, pp. 1003–1009, 2000.

[11] B. Hannaford and J. Ryu, "Time-domain passivity control of haptic interfaces," *IEEE Transactions on Robotics and Automation*, vol. 18, no. 1, pp. 1–10, 2002.

[12] K. Hertkorn, T. Hulin, P. Kremer, C. Preusche, and G. Hirzinger, "Time domain passivity control for multi-degree of freedom haptic devices with time delay," in *2010 IEEE International Conference on Robotics and Automation (ICRA)*. IEEE, 2010, pp. 1313–1319.

[13] J. Ryu, C. Preusche, B. Hannaford, and G. Hirzinger, "Time domain passivity control with reference energy following," *IEEE Transactions on Control Systems Technology*, vol. 13, no. 5, pp. 737–742, 2005.

[14] D. Lee and K. Huang, "On passive non-iterative variable-step numerical integration of mechanical systems for haptic rendering," in *ASME Dynamic Systems & Control Conference*, Ann Arbor, Michigan, USA, October 2008.

[15] J. Brown and J. Colgate, "Minimum mass for haptic display simulations," in *ASME Dynamic Systems and Control Division*, 1998.

[16] R. Ellis, N. Sarkar, and M. Jenkins, "Numerical methods for the force reflection of contact," *ASME Trans. Dyn. Syst. Meas. Control*, vol. 119, pp. 768–774, 1997.

[17] V. Chawda and M. OMalley, "On the performance of passivity-based control of haptic displays employing Levants differentiator for velocity estimation," in *2012 IEEE Haptics Symposium*, Vancouver, BC, Canada, March 2012.

[18] J. Ryu, Y. Kim, and B. Hannaford, "Sampled-and continuous-time passivity and stability of virtual environments," *Robotics, IEEE Transactions on*, vol. 20, no. 4, pp. 772–776, 2004.

[19] A. Mohtat and J. Kövecses, "Energy-consistent force feedback laws for virtual environments," *to appear in ASME J. Computing and Information Science in Engineering*, 2013. doi: 10.1115/1.4023918.